

Iranian Journal of Hydrogen & Fuel Cell

IJHFC

Journal homepage://ijhfc.irost.ir



Morphological and physical study of Cu-Ni sintered porous wicks used in heat pipes and fuel cells

M. Moayeri¹, A. Kafrou^{1*}, D. Sadeghi Fateh²¹Department of Advanced Materials and Renewable Energy, Iranian Research Organization for Science and Technology, Tehran, Iran²Department of Chemical Industry, Iranian Research Organization for Science and Technology, Tehran, Iran

Article Information

Article History:

Received:

16 Oct 2016

Received in revised form:

14 Jan 2017

Accepted:

17 Jan 2017

Keywords

Copper-Nickel powder

Sintered porous wicks

Porosity

Permeability

Heat Pipe & Fuel cell

Thermal Conductivity

Abstract

Recently, the use of renewable energies has increased to environmental pollution, limitation of fossil energy resources and energy security. One of the means that enable us to use such energies is fuel cells (FC). However, there are many problems in the commercialization of FC from an economically and operation perspective. One of the most important problems is heat management. New heat pipes are being developed for this purpose. A heat pipe is made from a "porous coat" on a base metal. In this study, a Cu-Ni porous layer with a thickness of $\sim 300\mu\text{m}$ was considered as the coating on a Cu-Ni base metal with two kinds of powder (mixed and ball milled). The morphology and physical properties of the coatings, such as porosity, permeability and effective thermal conductivity, were investigated. The best permeability was obtained for the base metals coated with powder which was ball milled for 6 hours. Thermal conductivity of samples increased (by 9.5%) when using ball milled powder. Porosity of coated samples decreased with ball milled powder in comparison to mixed powder.

1. Introduction

Recently, the use of renewable energies have attracted a great deal of research due to environmental pollution, exploitation of fossil energy resources and energy security. Fuel cells are the means that can help us achieve these goals. But, many technological

problems, such as thermal management, must be solved for FC before they can be commercialized [1-5].

A PEM fuel cell operates normally in a temperature range of 60-80 °C [6]. This range is determined by the materials of the PEM: anode, cathode, electrolyte, etc. In order to achieve high proton

conductivity in the electrolyte, the temperature must not exceed approximately 80 °C [7]. So, proper thermal management is one of the most critical technical problems that must be resolved [8-10]. The heat generated in a PEMFC can be removed by the cooling system or transferred by conduction–convection across the faces of the stack (bipolar plate) [11]. In a previous studies a novel design was proposed in which the bipolar plates are fabricated from a porous, hydrophilic material (so called heat pipe) [1, 12]. A heat pipes includes a metal sintered powder wick or a silicon/carbon porous wafer with biporous (micro/macro) pores on the inner/outer surface of a tube that is saturated with working fluid. Heat pipes with extremely high thermal conductivity, insensitive to gravity forces, high permeability for fluids, and a small cross-sectional area can transport large amounts of heat over a large distance [13].

The optimized heat transfer objectives can usually be stated as either a) removing large rates of energy generation through small surface areas with moderate surface temperatures rises or b) reducing the size of a boiler for a given rate. Both objectives involve higher heat fluxes [2, 14, 15].

The history of this method of heat transfer goes back to 1956 when pioneer Milton studied the porous surface layer for heat transfer and filed the first patent on sintering porous surface material (heat exchange systems) [16]. This technique was further developed in the 1970s by several researchers [17-19].

The porous layers being applied on tube surfaces can be classified based on their manufacturing methods to: sintering, thermal spraying, electrolytic plated, etc. Among these the sintering porous surface has been reported to give the best heat transfer ratio [15, 17, 20, 21]. In fact, the critical heat flux rate per unit area of the porous surface tubes can be 3-8 times more than reference smooth tubes [21-23]. They not only enhance the boiling coefficient of heat transfer, but also reduce the boiling temperature [24-26]. For example, the nanoporous Al_2O_3 structure showed significant enhancement of boiling heat transfer even throughout a 500 hour long-term pool-boiling test [26]. Sintered wicks using copper powders have been

found to exhibit the best available heat flux performance. Sintered copper has a heat flux capacity of 100 W/cm². By incorporating a naturally pulsating mechanism in the partially sintered copper wicking medium, a heat flux as high as 220 W/cm² has been achieved [19].

Nevertheless, there are some disadvantages in conventional processes, i.e., high temperature and long sintering time, which can affect the microstructure, heat resistance, and shape of the tubes. Therefore, it is generally recommended to develop an improved production process and select an optimum condition process [27, 28].

The porous surface promotes a large number of nucleation sites [2, 20, 23-24]. It is well known that the surface structure affects the pool boiling heat transfer from a heated surface [2, 18, 22, 26]. The number and size distribution of cavities present on a heated surface affect the nucleation characteristics [19]. The connection between particles in porous layers and the size of the channels are the two factors which depend on the powder shape, powder size and sintering conditions [3, 17, 19, 23, 29, 30].

The aim of this study is to establish micro-scale porous structures of Cu-Ni on the surface of a Cu-Ni base plate to improve thermal control in the fuel cell stack. For this purpose, the received mixed and mechanical alloyed powders of Cu-10% Ni were coated on the surface of plates without any pressure using a polymeric binder. The samples were dewaxed and then subjected to a special sintering. Micro structure and physical properties of the samples, such as porosity and permeability, were then characterized.

2. Experimental procedure

(a) Sample preparation

Commercial copper and Nickel powders from Powder Metallurgy Co. Iran were prepared. The average particle size of the powders were 100 μm for copper and nickel (Fig.1). Complete specifications are shown in Table 1.

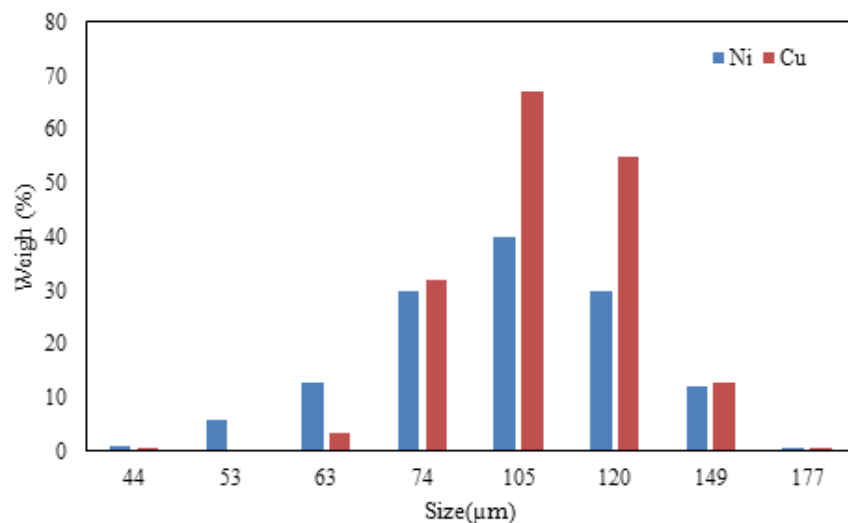


Fig. 1. Sieve analyses of Cu-Ni powders.

Table.1. Copper and Nickel powder specifications

Powder	Cu	Ni
Shape	Irregular	Sponge
Particle Size, (μm)	100±10	100±10
Purity (wt %)	99.5	99
Product method	Water Atomized	Thermo-Chemical Reduction

The morphology of the received powders was determined by a MIRA TESCAN scanning electron microscopy (SEM) (Fig. 2). SEM uses a finely focused beam of electrons in order to produce a high resolution image of a sample. These observations confirmed that the geometry of the copper powder is irregular and the nickel powder is sponge shape. X-ray diffraction (XRD) analysis was carried out for deter-

mining the existing phases using an EQuniox-3000 with Cu- α radiation. Fig. 3 shows this pattern. It is clear that the copper and nickel are the main elements of the powders.

Ball milling (BM) was performed in a high energy planetary ball mill (PM 200 Retch) under an argon atmosphere (99.99%) for various times of 2-12 hours. A stainless steel hardened vial and balls (65

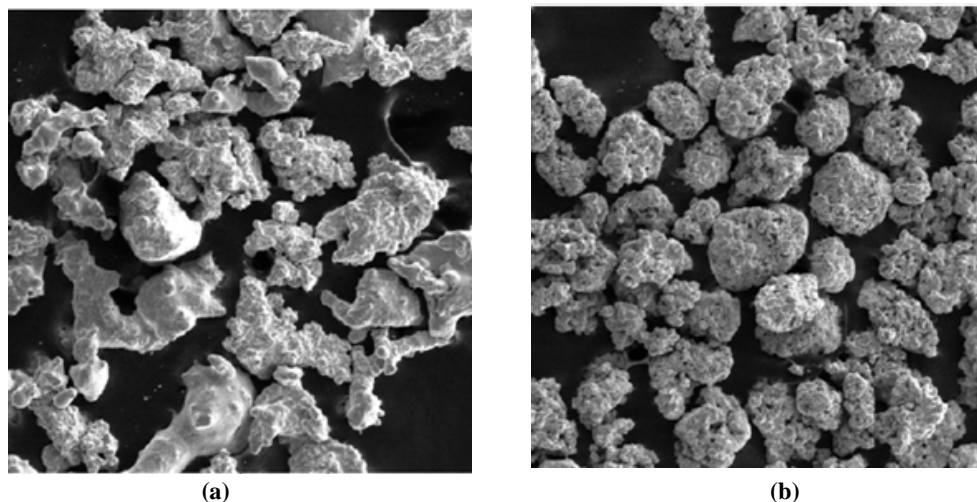


Fig. 2. SEM Micrograph of the received a) Cu and b) Ni powders ($\times 200$).

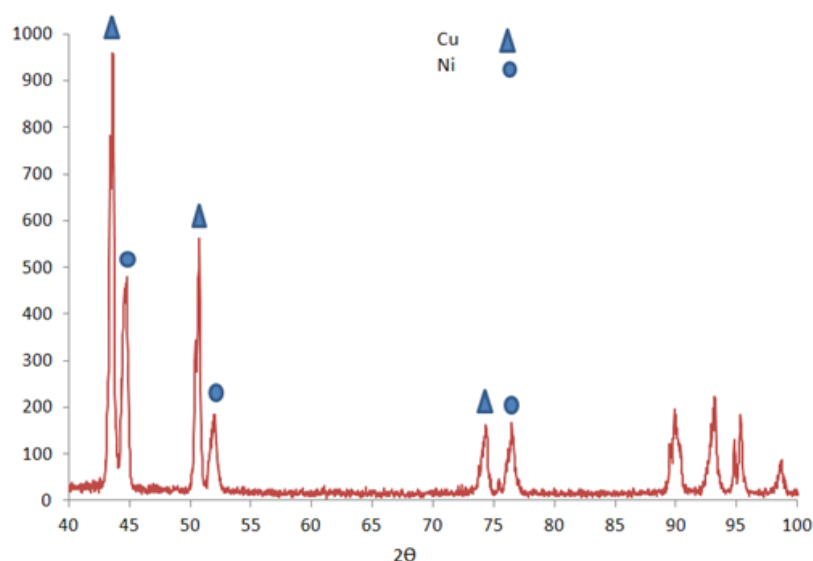


Fig. 3. XRD patterns of the received Mixed Cu-Ni powder.

RC hardness, 10 mm diameter) were used with a ball to powder weight ratio of 10:1. The copper to nickel powder weight ratio was set to 9:1. In addition, about 0.1% wt of load stearate was added to prevent the agglomeration and cold welding of powder particles. In order to study the phase formation during the milling process, a small amount of the powder was taken out from the vial at different intervals. After milling, the powder was classified and an appropriate particle distribution for coating was attained by mechanical sieving according to ASTM B214-07 [31]. Scanning electron microscopy was also used to determine the particle morphology. Also, a mixed Cu-Ni powder in a 9:1 weight ratio without any additional working was used for coating and the results were compared with BM coated powders.

A propylene binder was poured on the Cu-Ni plate (dimension of the plate was selected at 10*10 mm) and then the received and BM powders were sprinkled on it (with an amount of 0.35 gr/cm² of the metallic powders). This process was repeated at least three times to achieve a certain thickness (200-300 μm, the size of 2-3 adhered particles). This range is an effective coating thickness for porous wicks used in heat pipes [32].

The samples were heated in a Memert oven at 250 °C for 2 hours to remove the water. Dried samples were then heated for 30 minutes at 300 °C to remove the latex composition of the binder. At this temperature

the binder evaporated completely without any destructive effect on the coating. Coated plates were heated up to 950°C for 90 min. The sintering process is shown in Fig. 4. The heat treatment was carried out in a programmable atmosphere controlled tube furnace. Before starting the process, reduction gas (5% Hydrogen-95% N₂) was purged from the furnace for 10 minutes, this also occurred during the sintering process.

(b) Characterization

As described by Darcy's law, permeability is the capacity of a porous medium to transmit fluid and depends on the fluid medium. The hydraulic conductivity of the porous medium is examined first and then transformed into permeability. The hydraulic conductivity of porous samples can be determined by [25]:

$$K = \frac{qL_m}{hAt} \quad (1)$$

where K is the equivalent hydraulic conductivity of a porous medium, q is the cumulative quantity of deionized water, L_m is the specimen thickness, h is the difference in hydraulic head across of the specimen, A is the cross-sectional specimen area, and t is the total time. The permeability of a porous medium can be calculated from Eq. (2):

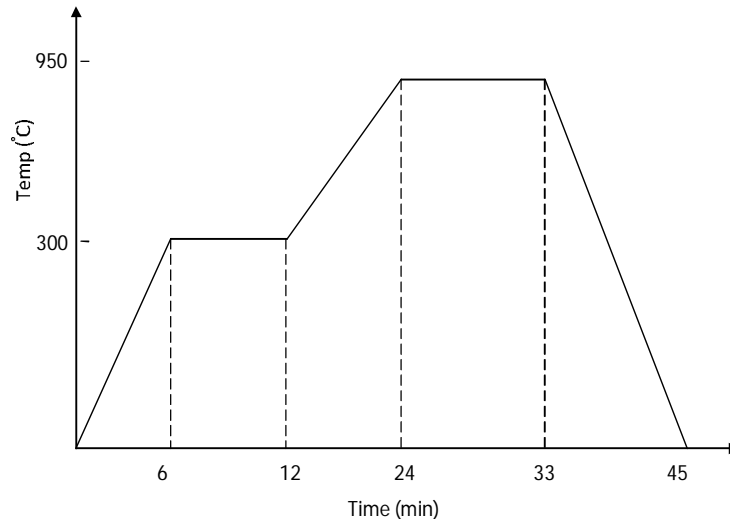


Fig. 4. A typical heat treatment cycle of the specimens.

$$P = K \frac{\mu_T V_{20^\circ\text{C}}}{\mu_{20^\circ\text{C}} g} \quad (2)$$

where μ_T is the water viscosity at testing temperature, $\mu_{20^\circ\text{C}}$ is the water viscosity at 20 °C, g is the acceleration due to gravity, and $V_{20^\circ\text{C}} = 1 \times 10^{-6} \text{ m}^2/\text{s}$ is the kinematic viscosity of deionized water at 20 °C. To measure the porosity a porous tablet was made with the same sintering condition. The porous specimens were saturated with methyl alcohol and porosity, ε , was measured by Eq. (3).

$$\varepsilon = \frac{(W_F - W_T) / \rho_L}{(W_T / \rho_m) + ((W_F - W_T) / \rho_L)} \quad (3)$$

Where W_T is the mass of the Cu-10% Ni porous tab, ρ_m is the intrinsic density of the Cu-10% Ni powder, W_F is the mass of the methyl alcohol-wetted wick, and ρ_L is the density of methyl alcohol. The experimental uncertainty in the porosity was estimated to be $\pm 1.0\%$. Details of the characterization of the porous layer is explained in [33].

3. Results and discussion

3.1. Phase definition

Fig. 5 presents the XRD patterns of the Copper and Nickel milled for 2, 6 and 12 hours. As it can be seen, a Ni peak exists after 2 hours. At other milling times

the peaks of Cu and Ni elements are eliminated. During milling, because of the intrinsic properties of a planetary mill, powder particles are subjected to high-energy impact which causes cold welding and fracture of powder particles [34]. The preliminary experiments revealed that both fcc Cu and fcc Ni peaks diminished after 6 hours milling and issued formation of a single fcc phase, which suggests a CuNi solid solution bimetallic phase. The XRD results indicate the direct formation of CuNi alloy in the milling process. In addition, the Bragg peak broadening (corresponding to the grain size reduction and micro strain accumulation in the lattice) is observed with increasing milling time. Reduction of peak intensity occurred as milling time increased, pointing out the increase in the Cu–Ni phase lattice parameter [35]. Based on the XRD analysis, further milling revealed no significant changes in the X-ray diffraction pattern of the powder (Fig. 5); so, 6 hours ball milling can be considered as the suitable condition.

3.2 Morphologies of ball milled powder and sintered coatings

SEM micrographs of the Cu and Ni powders milled for different times are presented in Fig. 6. These pictures clearly demonstrate the changes of powder morphology with increasing milling time. Powders milled for 2 hours have a disk-like morphology (Fig. 6a).

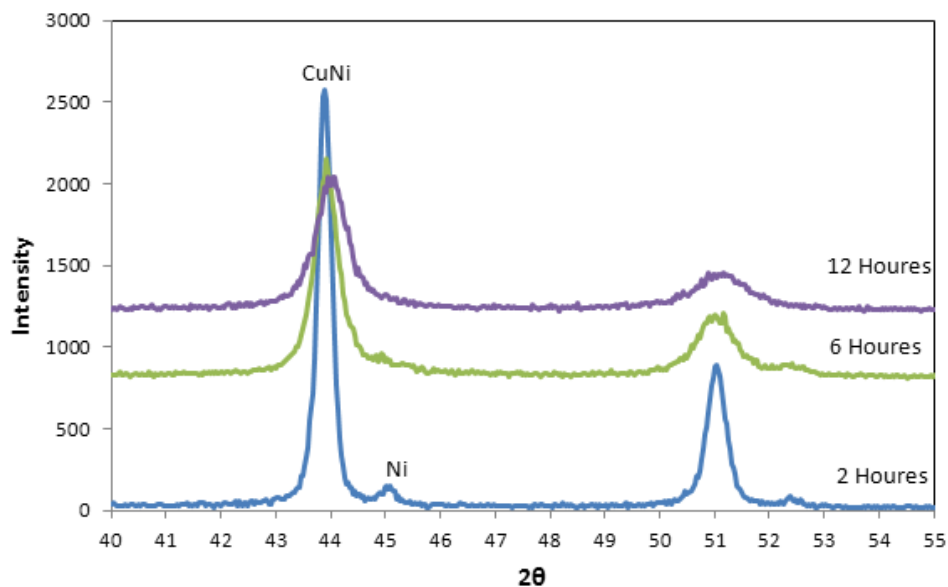


Fig. 5. XRD patterns of Cu - Ni samples milled for different times.

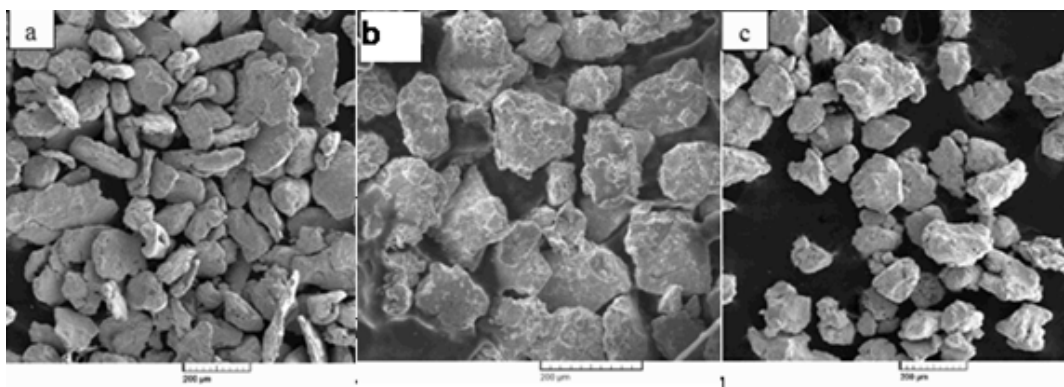


Fig. 6. Morphology of powders milled for a) 2 h, b) 6 h, and c) 12 h ($\times 200$).

By increasing the milling time (Fig. 6b and Fig. 6c), powders change to anirregular-spherical and agglomerated morphology. Compared to Fig. 2, agglomerations of ball milled powders are quite noticeable.

Fig. 7 illustrates the surface morphology of coatings obtained by applying milled powders after the sintering process. It can be seen that the shape of grains are irregular-spherical in samples coated with 12 hour milled powder. Comparing milled samples with the mixed one, the latter has more porosity (Fig. 7d). From this point of view, the surface obtained by the as received mixed powder is better than BM, but it must be noted that some places on the coating with mixed powder are Ni poor as shown in the EDS analysis in Fig. 8. This deficiency has a

significant effect on the mechanical properties [36] and corrosion resistance of the coating [24].

Fig. 9 illustrates a cross section view of the samples and shows that there is a kind of reentrant cavity with a larger internal surface. This type of coating is suitable for heat transfer purpose because it facilitates fluid penetration and boiling nucleation [27, 30].

Observation on a cross section of coatings revealed that just mixed powder and milled powder for 6 hours, had larger and more interconnected pores. These parameters are very important for heat transfer properties [2, 15, 17, 19-21, 27]. Comparing the disk-like and irregular-spherical powder (Fig. 10) shows that the latter has more interconnected pores because of the particle shape and surface contact between grains.

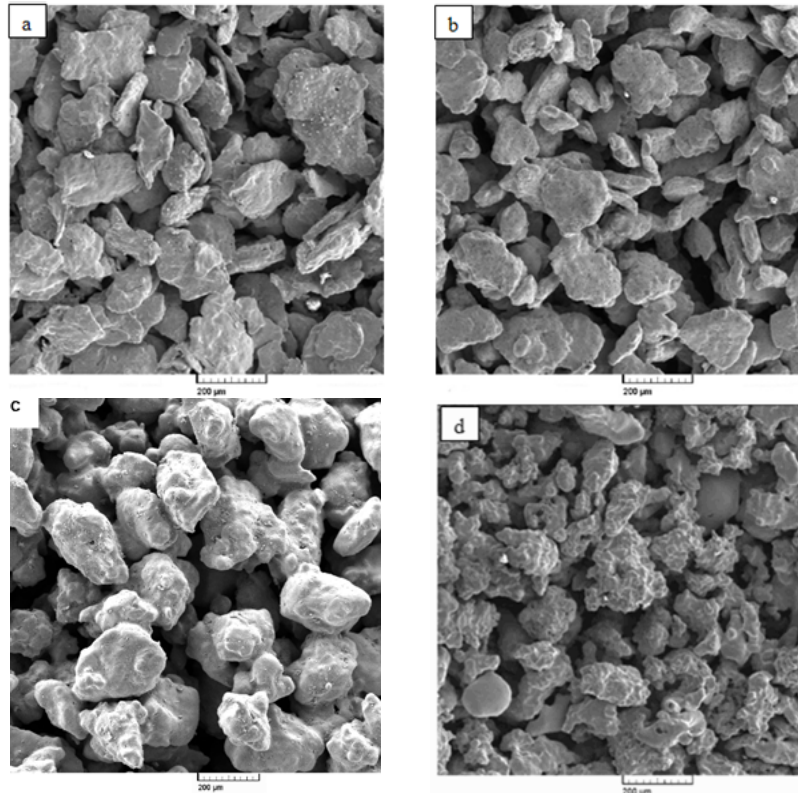


Fig. 7. SEM micrograph of coats (top view) (sintered at 950 °C for 90 min), milled for a) 2 h, b) 6 h, c) 12 h, and d) Mixed powder (×200).

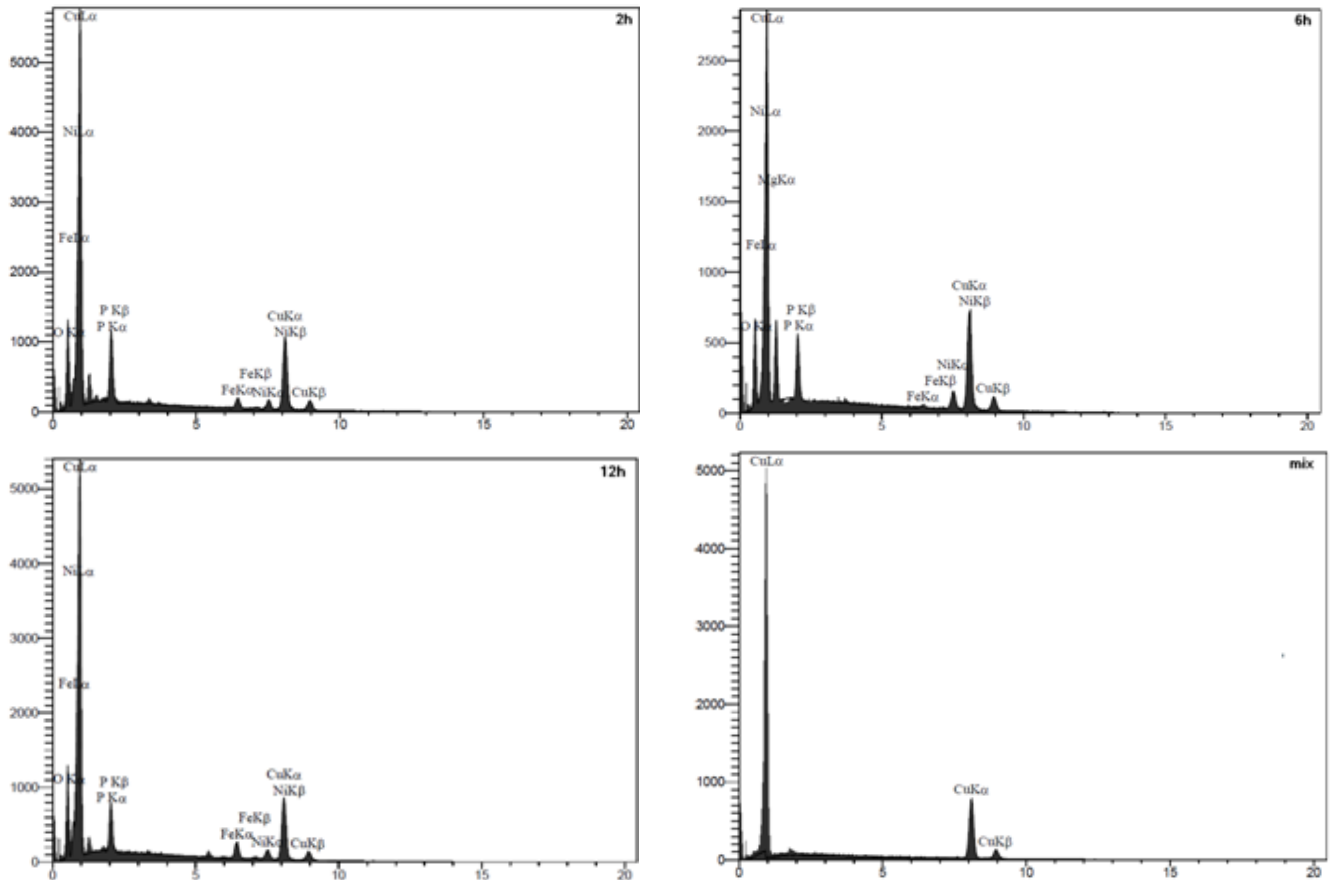


Fig. 8. Energy dispersive spectroscopy (EDS) analyses of coats obtained with different BM and mixed powders.

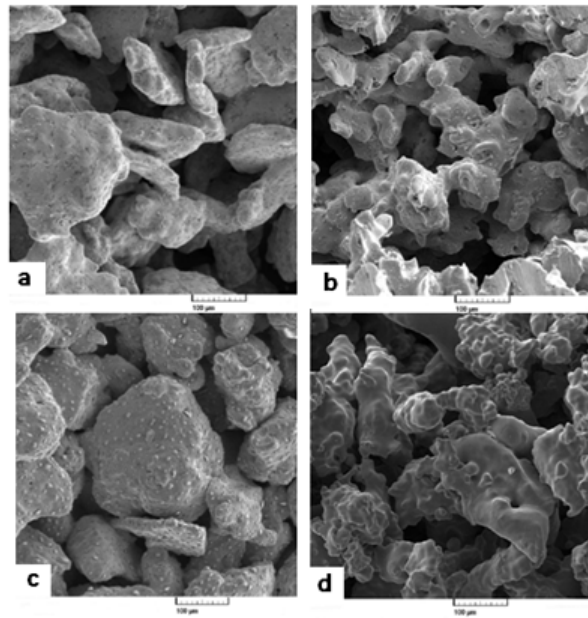


Fig. 9. Cross section view of coats milled for a) 2 h, b) 6h, c) 12 h, and d) Mixed powder ($\times 800$).

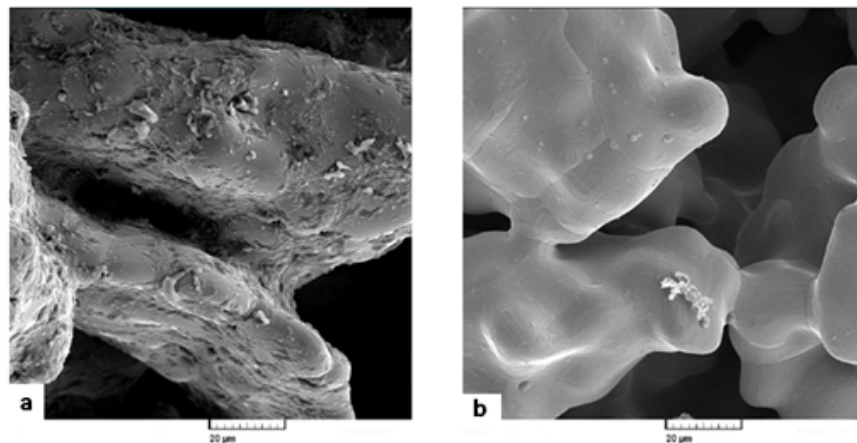


Fig. 10. Joining of two neighbor particles after sintering a) disk like (BM) and b) irregular-spherical shape (mixed).

In the coats created by the received mixed powder the surface of the channels are smooth; however in the BM cases it was not smooth.

3.3 Porosity

In our experiments, the porosity of the sintered coating varies from 32.6 to 42.3% (Table 2). However, the porosity of previous research is generally not more than 50% [37-38]. From Table 2 it can be seen that the highest value of porosity belongs to the mixed powder and lowest value for belongs to 12 hours BM powders. These variations can be related to the morphology of the powders at different milling times as powder shape and mode of connection has a direct

effect on porosity volume. The coatings are more compact in the case of 12 hours BM powders. It seems that high energy mechanical milling provides residual stress in powders (according to Fig. 5. and the main peaks move to the right with increased milling time) and causes decreasing sintering temperature [39]. So, increased milling time lessens the porosity in samples. As many researchers have stated, the best efficiency of porous layers in heat transfer equipment is achieved with 35-45% porosity with connecting channels in the coating layer [40-43], in our study the results for 6 hours BM powder met this condition. After 6 hours ball milling the powder shape changed from a disk-like to an irregular-spherical morphology, good diffusion happened between the powders, and

Table 2. Physical properties of sintered coating

Sample	2h	12h	6 h	Cu-Ni Mix
Porosity (%)	36.3	32.6	34	42.3
Permeability (cm) ² ×10 ⁻⁸	1.7	1.8	2.1	1.92
K _{eff} (W/m.K)	27.7	28.8	28.3	26.1

a netlike porosity formed after sintering (Fig. 9). Also, net-like porosity formed in the mixed powder because of its irregular-spherical shape and good bonding between particles.

3.5 Thermal conductivity

The thermal conductivity of the sintered porous coating is related to its porosity through the following equation [25]:

$$k_{eff} = k_s \left[\frac{2 + k_{air}/k_s - 2\varepsilon(1 - k_{air}/k_s)}{2 + k_{air}/k_s + \varepsilon(1 - k_{air}/k_s)} \right] \quad (4)$$

Where k_{eff} is the effective thermal conductivity of the sintered wick, k_s is the intrinsic thermal conductivity of Cu-10% Ni solid, k_{air} is the intrinsic thermal conductivity of air and ε is the porosity of the sintered coating. Calculated results are summarized in Table 2. According to equation (4) porosity is the most important parameter that affects thermal conductivity. Ignoring the morphology of the powder, the coating with 12 hours ball milled powder that presents less porosity has more thermal conductivity and the mixed powder with 42.3% porosity has less thermal conductivity.

3.6 Permeability

For better performance of a porous layer, the pore size must be small enough to ensure high capillary pressure to draw the fluid through the porous coating, sometimes even against gravity [27]. Table 2 shows the permeability value of the coatings. These amounts are higher for 6 hours BM powder.

Many researchers have shown that besides porosity, there are also other factors that may affect the performance of the porous coatings [22-24]. This accorded well with the literatures which have

reported that samples with the same porosity may also have different permeability [26].

Since all coatings were made in the same conditions, the difference in the permeability value is related to the powder morphology, porosity value, pore size and pore surface roughness. There was a good connection between powders after sintering, and as a result good net-like porosity for irregular-spherical powder causes good permeability. The results were comparable with other researcher such as Dominguez [17], Chiu [20] and Peterson [25]. As mentioned before, adjustment of all properties for these kinds of coatings, is a very important parameter in the design. Irregular particles with more connection channels have shown better permeability. For 2 hours and 12 hours BM, permeability values were less than for mixed and 6 hours BM coatings. Disk-like (BM for 2 hours) and agglomerated (BM for 12 hours) morphology made disconnected pores and so less permeability (Fig. 9 and Fig. 10). Also, in these two cases much rougher powder and channel surfaces was obtained compared to 6 hours BM and mixed coatings. These morphology differences caused the difference in the effective pore size, as illustrated in Fig. 9 and 12 hours BM had a smaller pore size, while the 6 hours and mixed had a larger and a slightly narrower pore size distribution.

As mentioned above, the surface of wall pore for 6 hours BM was rougher than the mixed wall. Surface roughness decreases the contact angle between the fluid and surface, and consequently increases permeability [44-45], so the 6 hours BM powder showed more permeability. As can be seen in Fig.9, this is also induced by the significantly larger pore size in the 6 hours BM powder.

4. Conclusion

In this research a morphological and physical study of Cu-10%Ni sintered porous wicks used in fuel cells was done and the following conclusions can be drawn :

1. Porosity volume in coatings with BM was less

than coated samples with as received mixed powder so the thermal conductivity of BM samples is more than mixed samples.

2. Higher permeability was achieved for 6 hours BM loose sintering powder created at 950 °C. In this case, pore wall surface roughness, powder morphology and interconnectivity of channels are suitable for heat enhancement surfaces. Surface roughness of the BM powder was more than the mixed powder. Surface roughness decreases the contact angle between the fluid and surface and consequently increases the permeability of wicks.

3. Thermal conductivity of samples increased (by 9.5%) when using ball milled powder.

Acknowledgments

The authors would like to express their gratitude to the Arac Petrochemical Company (APC) for their financial support.

References

- [1] Faghri A., Z. Guo., "Challenges and opportunities of thermal management issues, related to fuel cell technology and modeling", *Int. J. Heat Mass Tran.*, 2005,48: 3891.
- [2] Faghri A., "Heat pipe science and technology", Taylor & Francis, Washington, DC. 1995.
- [3] Holley B. and Faghri A., "Permeability and effective pore radius measurements for heat pipe and fuel cell applications", *Applied Thermal Engineering*, 2006, 26:448.
- [4] Garrity P.T, Klausner J.F. and Mei. R, "A flow boiling microchannel evaporator plate for fuel cell thermal management", *Heat Transfer Engineering*, 2007, 28: 877.
- [5] Izenon M. G. and Hill R. W., "Water and Thermal Balance in PEM Fuel Cells". *Journal of Fuel Cell Science and Technology*, 2004, 1: 10.
- [6] Kandlikar S. G. and Lu Z., "Thermal management issues in a PEMFC stack – A brief review of current status", *Applied Thermal Engineering*, 2009, 29: 1276.
- [7] Freire T.J.P. and Gonzalez E.R., "Effect of membrane characteristics and humidification conditions on the impedance response of polymer electrolyte fuel cells", *J. Electroanal. Chem*, 2001, 503: 57.
- [8] Goebel S.G." Evaporative cooled fuel cell", US Patent 6,960,404, 2005.
- [9] Shimoi R., Masuda M., Fushinobu K., Kozawa Y. and Okazaki K. "Visualization of the membrane temperature field of a polymer electrolyte fuel cell", *J. Energy Resource Technol*, 2004, 126: 258.
- [10] Bvumbe T. J., Bujlo P., Tolj I., Mouton K., Swart G., Pasupathi K. and Bruno G., "Review on management, mechanisms and modeling of thermal processes in PEMFC", *Hydrogen and Fuel Cells*, 2016, 1:1.
- [11] Brambilla M. and Mazzuchelli G., "Fuel cell with cooling system based on direct injection of liquid water", US Patent 6835477, 2004.
- [12] Matsuzaki T., "Cooling system for fuel cell and prevention method for degradation of coolant therefore", US Patent 7160468, 2007.
- [13] Leonard. L. Vasiliev and Leonid L. Vasiliev, "Heat pipes to increase the efficiency of fuel cells", *Int. J. of Low Carbon*, 2008,4: 96.
- [14] Madhusudana R. S. and Balakrishnan A. R., "Analysis of pool boiling heat transfer over porous surfaces", *Heat and Mass Transfer*, 1997, 32: 463.
- [15] Li J., Zou Y., Cheng L., Singh R. and Akbarzadeh A., "Effect of fabricating parameters on properties of sintered porous wicks for loop heat pipe", *Powder Technology*, 2010, 204: 241.
- [16] Milton R. M., Heat exchange system, US3384154,

1968.

[17] Dominguez F. A., Peters T. B. and Brisson J. G., "Effect of fabrication parameters on the thermophysical properties of sintered wicks for heat pipe applications", *Int. J. of Heat and Mass Transfer*, 2012, 5: 7471.

[18] Jiang Y.Y., Wang W.C., Wang D. and Wang B.X., "Boiling heat transfer on machined porous surfaces with structural optimization", *Int. J. of Heat and Mass Transfer*, 2001, 44: 443.

[19] Zuo, Z. J., North M.T., and Wert, K. L., "High heat flux heat pipe mechanism for cooling of electronics". *IEEE Transactions on Components and Packaging Technologies*, 2001, 24: 220.

[20] Chiu L.H., Wu C.H., Lee P.Y., "Comparison between oxide-reduced and water-atomized copper powders used in making sintered wicks of heat pipe", *China Particuology*, 2007, 5: 220.

[21] Xiao Z., and Zhao Y., "Heat Transfer Coefficient of Porous Copper with Homogeneous and Hyride Structure in Active Cooling", *J. Mater. Res*, 2013, 28: 2545.

[22] Li C. H., Li T., Hodgins P., Hunter C.N., Voevodin A. A. and Jones J. G., "Comparison study of liquid replenishing impacts on critical heat flux and heat transfer coefficient of nucleate pool boiling on multiscale modulated porous structures", *Int. J. of Heat and Mass Transfer*, 2011, 54: 3146.

[23] Furberg R., Palm B., "Boiling heat transfer on a dendritic and micro-porous surface in R134a and FC-72", *Applied Thermal Engineering*, 2011,31: 3595.

[24] Lin Y-J. and Hwang K-S., "Swelling Of Copper Powders During Sintering Of Heat Pipes In Hydrogen-Containing Atmosphere", *Materials transactions*, 2010, 51: 2251.

[25] Peterson G. P. and Fletcher L. S., "Effective thermal conductivity of sintered heat pipe wicks", *J. of*

Thermophysics, 1987, 1: 343.

[26] Kang M.G., "Effect of surface roughness on pool boiling heat transfer", *Int. J. of Heat and Mass transfer*, 2000, 43: 4073.

[27] Sarwar M.S., Jeong Y.H. and Chang S.H., "Subcooled flow boiling CHF enhancement with porous surface coatings", *Int. J. Heat and Mass Transfer*, 2007,50: 3649.

[28] Li J., Yong J., Cheng L., Singh R. and Akbarzadeh A. "Effect of fabricating parameters on properties of sintered porous wicks for loop heat pipe", *Powder Technology*, 2010, 204: 241.

[29] Faghri A. and Guo Z., "Integration of Heat Pipe into Fuel Cell Technology", *Heat Transfer Engineering*, 2008, 29: 232.

[30] Cieśliński J. T., "Nucleate pool boiling on porous metallic Coatings", *Experimental thermal and fluid science*, 2002, 25: 557.

[31] ASTM B214-07, Standard Test Method for Sieve Analysis of Metal Powders, 2011 ASTM.

[32] Yang C-Y and Liu C-F, "Effect of coating layer thickness for boiling heat transfer on micro porous coated surface in confined and unconfined spaces", *Experimental Thermal and Fluid Science*, 2013, 40: 47.

[33] Moayeri M. and Kafrou A., Effect of powder shape on effective thermal conductivity of Cu-Ni Porous Coatings, *J. of Materials Research and Technology*, 2017, in press.

[34] Callister W. D., "Fundamentals of Materials Science and Engineering", 5th edn, John Wiley & Sons, New York, 2001, 287.

[35] Durivault L., Brylev O., Reyter D., Sarrazin M., Bélanger D. and Roué L., "Cu-Ni materials prepared by mechanical milling: their properties and electrocatalytic activity towards nitrate reduction in alkaline medium", *Journal of Alloys and Compounds*, 2007, 432: 323.

[36] Angelo P. C. and Subramanian R., "Powder Metallurgy: Science, Technology and Applications", Publisher: Phi Learning, 2008.

[37] Khan A.F. and Patil A. P., "Combined effect of chloride and pH on corrosion resistance of Cu-10Ni alloy", Transactions of the Indian Institute of Metals, 2008, 61: 225.

[38] Thewsey D.J and Zhao Y.Y., "Thermal conductivity of porous copper manufactured by the lost carbonate sintering process", physica status solidi (a), 2008, 205: 1126.

[39] Forrseter J. S., Gooddhaw H. J., Kisi E. H., Suaning G. J. and Zobec J. S., J. Aust. Ceram. Soc. 2008, 44: 52.

[40] Wu W., Du J-H., Hu X-J. and Wang B-X., "Pool boiling heat transfer and simplified one-dimensional model for prediction on coated porous surfaces with vapor channels", Int. J. of Heat and Mass Transfer; 2002, 45: 1117.

[41] Liou J. H., Chang C. W., Chao C. and Wong S. C., "Visualization and thermal resistance measurement for the sintered mesh-wick evaporator in operating flat-plate heat pipes", Int J. of Heat and Mass Transfer; 2010, 53: 1498.

[42] Jiyuan X., Zou Y., Mingxiu F. and Cheng L., "Effect of pore parameters on thermal conductivity of sintered LHP wicks", Int. J. of Heat and Mass Transfer, 2012, 55: 2702.

[43] Hwang G-S. and Kaviany M., "Critical heat flux in thin, uniform particle coatings, Int. J. of Heat and Mass Transfer, 2006, 49: 844.

[44] Miwa M., "Effect of surface roughness on sliding angle of water droplets on super hydrophobic surface", Langmuir, 2000, 16: 5754.

[45] McHale J. P. and Garimella S. V., "Bubble nucleation characteristics in pool boiling of a wetting liquid on smooth and rough surfaces", Int. J. of Multiphase Flow, 2010, 36: 249.